

## Article

# Transcriptome Analysis Reveals the AhR, Smad2/3, and HIF-1 $\alpha$ Pathways as the Mechanism of Ochratoxin A Toxicity in Kidney Cells

Min Cheol Pyo, In-Geol Choi and Kwang-Won Lee \*

Department of Biotechnology, College of Life Science &amp; Biotechnology, Korea University, Seoul 02841, Korea; reve03@korea.ac.kr (M.C.P.); igchoi@korea.ac.kr (I.-G.C.)

\* Correspondence: kwangwon@korea.ac.kr; Tel.: +82-2-3290-3473; Fax: +82-2-927-1970

**Abstract:** Ochratoxin A (OTA) is a mycotoxin occurring in foods consumed by humans. Recently, there has been growing global concern regarding OTA toxicity. The main target organ of OTA is the kidney, but the mechanism underlying renal toxicity is not well known. In this study, human-derived proximal tubular epithelial cells, HK-2 cells, were used for RNA-sequencing (RNA-seq) and transcriptome analysis. In total, 3193 differentially expressed genes were identified upon treatment with 200 nM OTA in HK-2 cells; of these, 2224 were upregulated and 969 were downregulated. Transcriptome analysis revealed that OTA significantly affects hypoxia, epithelial-mesenchymal transition (EMT), apoptosis, and xenobiotic metabolism pathways in kidney cells. Quantitative real-time PCR analysis showed gene expression patterns similar to RNA-seq analysis. Expression of EMT markers (E-cadherin and fibronectin), apoptosis markers (caspase-3 and Bax), and kidney injury molecule-1 (KIM-1) was suppressed by inhibiting AhR expression using siRNA, and the related transcription factors, Smad2/3, and HIF-1 $\alpha$  were downregulated. Smad2/3 suppression with siRNA could inhibit fibronectin, caspase-3, Bax, and KIM-1 expression. Fibronectin, caspase-3, Bax, and KIM-1 expression could be increased with HIF-1 $\alpha$  suppression with siRNA. Taken together, these findings suggest that OTA-mediated kidney toxicity via the AhR-Smad2/3-HIF-1 $\alpha$  signaling pathways leads to induction of EMT, apoptosis, and kidney injury.



**Citation:** Pyo, M.C.; Choi, I.-G.; Lee, K.-W. Transcriptome Analysis Reveals the AhR, Smad2/3, and HIF-1 $\alpha$  Pathways as the Mechanism of Ochratoxin A Toxicity in Kidney Cells. *Toxins* **2021**, *13*, 190. <https://doi.org/10.3390/toxins13030190>

Received: 16 January 2021

Accepted: 5 March 2021

Published: 6 March 2021

**Keywords:** ochratoxin A; aryl hydrocarbon receptor; Smad2/3; hypoxia-inducible factor-1 $\alpha$ ; RNA-sequencing

**Key Contribution:** Ochratoxin A-regulated DEGs are associated with hypoxia, xenobiotic metabolism, EMT and apoptosis, and ochratoxin A damages the kidney by inducing hypoxia, EMT, and apoptosis through AhR-Smad2/3, HIF-1 pathways.

**Publisher's Note:** MDPI stays neutral with regard to jurisdictional claims in published maps and institutional affiliations.



**Copyright:** © 2021 by the authors. Licensee MDPI, Basel, Switzerland. This article is an open access article distributed under the terms and conditions of the Creative Commons Attribution (CC BY) license (<https://creativecommons.org/licenses/by/4.0/>).

## 1. Introduction

Ochratoxin A (OTA) is a mycotoxin that occurs naturally in fungi such as *Aspergillus spp.* and *Penicillium spp.* OTA is known to exist in a variety of food groups such as cereals, cocoa, coffee, nuts, milk, beer, and wine, which are frequently consumed in daily life [1,2]. OTA (C<sub>20</sub>H<sub>18</sub>O<sub>6</sub>NCl, molecular weight: 403.8) is a colorless, odorless, slightly water-soluble crystalline compound belonging to the para-chlorophenolic group that structurally contains a dihydroisocoumarin moiety linked by an amide bond to L-phenylalanine [3]. It is more stable to heat than other mycotoxins and is absorbed into the body through the gastrointestinal tract with food consumption. Ingested OTA is rapidly absorbed through the jejunum with a bioavailability of 97% [4]. OTA binds strongly to albumin in serum and has a very long half-life, eventually accumulating in the body [5]. OTA is one of the most harmful fungal toxins and is classified in Group 2B as a possible human carcinogen by the International Agency for Research on Cancer [6]. The nephrotoxicity, hepatotoxicity,

immunotoxicity, neurotoxicity, and genotoxicity of OTA have been reported in various animal species [7–9].

OTA has various possible targets such as the liver, immune system, heart and brain; however, owing to the function of the organ, its main target is the kidneys [10–12]. The kidneys balance the metabolism of salt and water, regulate the levels of electrolytes in blood, and play several important physiological roles including maintaining the stable composition of blood and secretion of hormones [13,14]. The kidneys also receive about 25% cardiac output and function to filter the equivalent volume of extracellular fluid from plasma. Further, the concentration of toxic substances is increased as water and solutes are reabsorbed in the process of removing waste from systemic circulation and excretion to urine. As a result, the risk of renal exposure to toxic substances is increased [15]. Due to the high renal blood flow per tissue weight, a relatively large amount of OTA is delivered to the kidneys compared to other organs [16]. Further, OTA accumulation in kidney tissues, especially through reabsorption, results in the highest concentration of OTA to be detected throughout the body [17].

Transcriptome sequencing (RNA-seq) technology has been used to evaluate and analyze the overall response caused by toxic substances or stressors [18,19]. Although there is a limitation of RNA-seq that not all RNAs have been used to produce proteins, the use of RNA-seq technology to analyze differentially expressed genes (DEGs) is a reliable method for understanding the interactions between specific molecules and for conducting research on the mechanisms that cause toxicity [20,21]. DEG analysis has become a valuable tool for studying molecular mechanisms in response to toxic substances including mycotoxins [22]. Transcriptome analysis studies on OTA have been performed in a variety of cell lines and mammalian model systems [23–25]. Therefore, much information about the mechanism of OTA toxicity in the kidney can be obtained through transcriptional profiles obtained using RNA-sequencing.

Although much is known about the renal toxicity of OTA such as inflammation, apoptosis and pyroptosis [26,27], studies on the mechanisms underlying renal toxicity are still insufficient. Therefore, in the present study, transcriptome analysis was used to estimate changes in renal damage in response of OTA. In this research, OTA-induced renal toxicity such as epithelial-mesenchymal transformation (EMT), apoptosis and hypoxia were investigated in human proximal tubular epithelial HK-2 cells.

## 2. Results

### 2.1. Analysis of DEGs

To elucidate the molecular mechanisms responsible for OTA toxicity to the kidneys, transcriptome sequencing and analysis were conducted in HK-2 cells. Differential gene expression analysis of HK-2 cells following OTA treatment resulted in a total of 3193 DEGs, of which 2224 were upregulated and 969 were downregulated (Figure 1). As shown in the scatter plot, the expression level of certain genes was significantly ( $p < 0.05$ ) different between the control group and the OTA-treated group, suggesting that the gene expression of HK-2 cells was affected by OTA (Figure 2).

### 2.2. Functional Annotation of DEGs

To further explain the molecular function of DEGs identified in HK-2 cells exposed to OTA, GO and KEGG enrichment analysis were performed. As shown in Figure 3A–C, in case of GO analysis for the upregulated and downregulated DEGs, there are three categories, biological process, molecular function, and cellular component, and the top 15 terms for each category are shown based on  $p$ -values  $< 0.05$  (Figure 3D). Representative subsets in the biological process include cell–cell adhesion, rRNA processing, and viral process; molecular functions include protein binding, poly(A) RNA binding, and cadherin binding involved in cell–cell adhesion. Cellular components include nucleoplasm, membrane, and cytosol. KEGG pathway analysis also showed the top 15 pathways. As shown in Figure 3D, protein processing in the endoplasmic reticulum, insulin resistance, thyroid hormone signaling

pathway, proteoglycan in cancer, renal cell carcinoma, adherent junction, and others were found. Among the various KEGG pathways, renal cell carcinoma was the pathway with the highest fold-enrichment value. This is also associated with hypoxia and EMT [28,29].

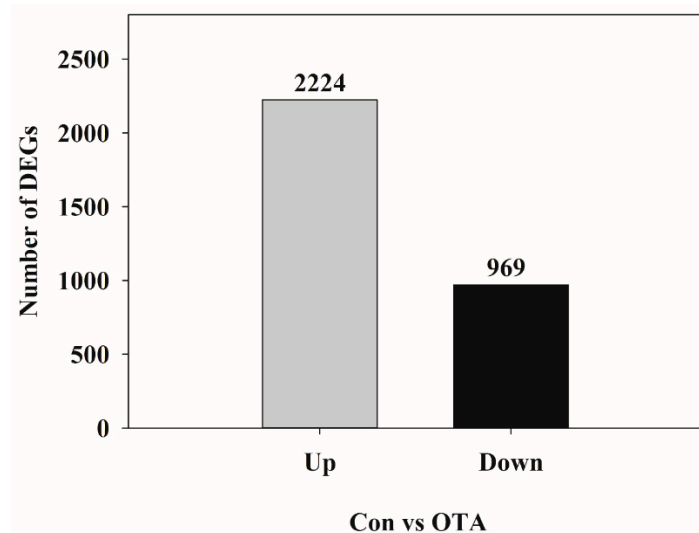


**Figure 1.** Statistical chart of showing the number of differentially expressed genes (DEGs) in ochratoxin A (OTA)-treated HK-2 cells compared to the control ones. Up represents upregulated DEGs, and Down represents downregulated DEGs. Con, control; OTA, ochratoxin A.

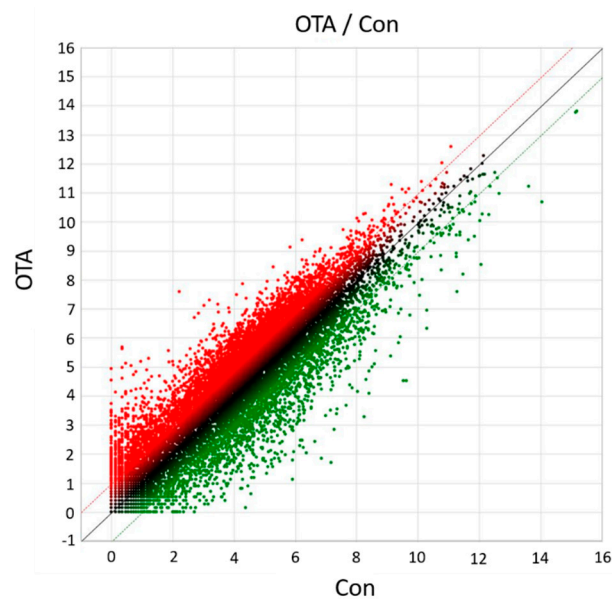


**Figure 2.** The scatter plot of DEGs between Con and OTA treatment groups. The X-axis indicates the log<sub>2</sub> expression values in Con group, and the Y-axis indicates the log<sub>2</sub> expression values in OTA group. Each point indicates a particular gene or transcript. Red dots indicate up-regulated genes, green dots indicate down-regulated genes, and black dots indicate genes showing nonsignificant changes.

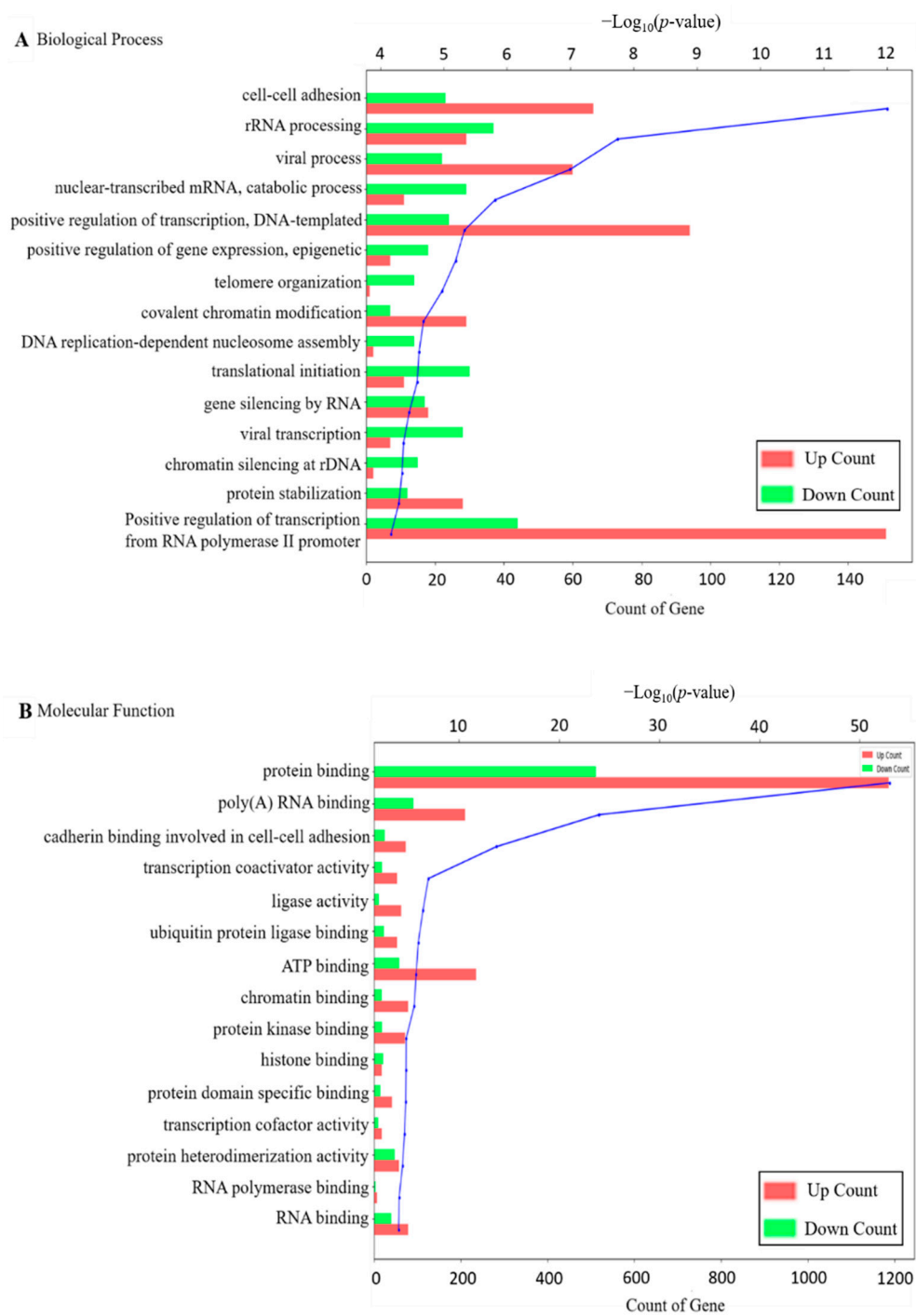
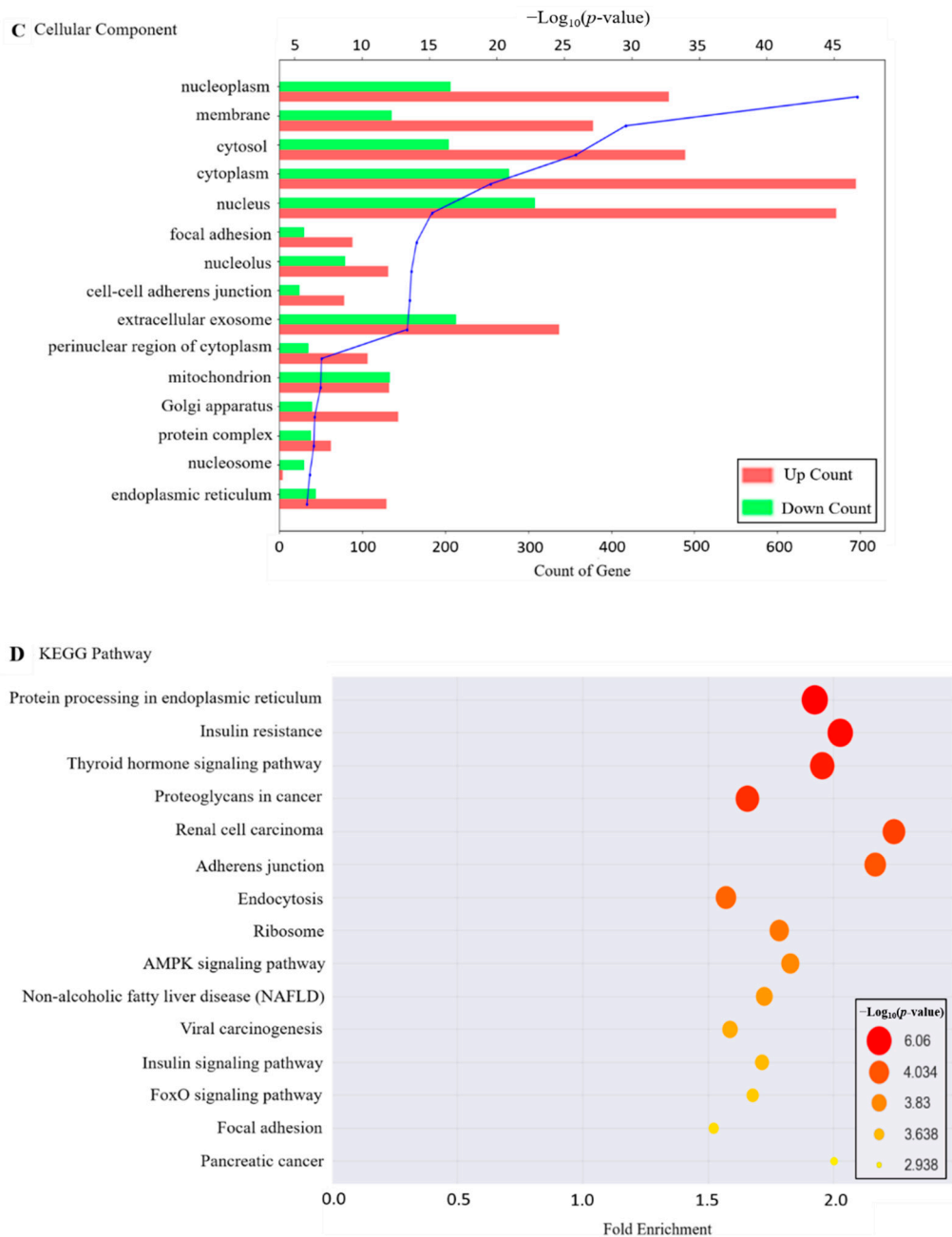


Figure 3. Cont.



**Figure 3.** Functional annotation of DEGs. Functional categories of DEGs, broadly separated into (A) biological process, (B) molecular function and (C) cellular component, based on Gene ontology (GO). The blue line of the graphs means  $-\log_{10}(p\text{-value})$ ; (D) Top fifteen enriched pathways in HK-2 cells exposed to OTA, analyzed by the KEGG pathway analysis ( $p < 0.05$ ), the size and color of the circle mean  $-\log_{10}(p\text{-value})$ . The position of the x-axis represents the degree of fold enrichment.

### 2.3. Gene Set Enrichment Analysis of Genes Related to OTA

To identify the potential functions of DEGs, GSEA was performed using the MSigDB hallmark gene set. As shown in Table 1, 20 gene sets regulated by OTA in HK-2 cells were identified. Among them, we focused on hypoxia, EMT, apoptosis, and xenobiotic metabolism as pathways for the toxic mechanism of OTA based on the results of KEGG analysis.

**Table 1.** Gene set enrichment analysis of genes related to OTA.

Gene Set Name	# Genes in Gene Set (K)	# Genes in Overlap (k)	k/K	p-Value	FDR q-Value
HYPOXIA	200	57	0.285	$1.02 \times 10^{-27}$	$5.09 \times 10^{-26}$
TNFA_SIGNALING_VIA_NFKB	200	50	0.250	$1.05 \times 10^{-21}$	$2.62 \times 10^{-20}$
EPITHELIAL_MESENCHYMAL_TRANSITION	200	46	0.230	$1.60 \times 10^{-18}$	$2.66 \times 10^{-17}$
GLYCOLYSIS	200	44	0.220	$5.26 \times 10^{-17}$	$6.58 \times 10^{-16}$
MTORC1_SIGNALING	200	43	0.215	$2.89 \times 10^{-16}$	$2.89 \times 10^{-15}$
UV_RESPONSE_DN	144	35	0.243	$3.19 \times 10^{-15}$	$2.65 \times 10^{-14}$
OXIDATIVE_PHOSPHORYLATION	200	40	0.200	$4.02 \times 10^{-14}$	$2.87 \times 10^{-13}$
UNFOLDED_PROTEIN_RESPONSE	113	29	0.257	$1.63 \times 10^{-13}$	$1.02 \times 10^{-12}$
ADIPOGENESIS	200	39	0.195	$1.96 \times 10^{-13}$	$1.09 \times 10^{-12}$
MITOTIC_SPINDLE	199	38	0.191	$7.86 \times 10^{-13}$	$3.85 \times 10^{-12}$
INFLAMMATORY_RESPONSE	200	38	0.190	$9.25 \times 10^{-13}$	$3.85 \times 10^{-12}$
P53_PATHWAY	200	38	0.190	$9.25 \times 10^{-13}$	$3.85 \times 10^{-12}$
INTERFERON_GAMMA_RESPONSE	200	35	0.175	$7.99 \times 10^{-11}$	$3.07 \times 10^{-10}$
ESTROGEN_RESPONSE_LATE	200	34	0.170	$3.30 \times 10^{-10}$	$1.18 \times 10^{-9}$
APOPTOSIS	161	30	0.186	$3.65 \times 10^{-10}$	$1.22 \times 10^{-9}$
TGF_BETA_SIGNALING	54	17	0.315	$5.17 \times 10^{-10}$	$1.61 \times 10^{-9}$
ESTROGEN_RESPONSE_EARLY	200	30	0.150	$6.75 \times 10^{-8}$	$1.88 \times 10^{-7}$
IL2_STAT5_SIGNALING	200	30	0.150	$6.75 \times 10^{-8}$	$1.88 \times 10^{-7}$
COAGULATION	138	24	0.174	$8.07 \times 10^{-8}$	$2.12 \times 10^{-7}$
XENOBIOTIC_METABOLISM	200	32	0.160	$1.86 \times 10^{-8}$	$4.05 \times 10^{-8}$

#### 2.4. Validation of Gene Expression Patterns Using qRT-PCR

To validate the transcriptome results of DEGs, qRT-PCR analysis was performed, and a total of 11 genes were selected based on the pathway results in the Hallmark gene sets through GSEA. Gene expression levels from qRT-PCR analysis showed similar trends and magnitudes of changes compared to the transcriptome analysis (Figure 4). Correlation analysis of the 11 DEGs yielded an  $R^2$  of 0.8097, demonstrating excellent linearity between the RNA-seq and qRT-PCR results, confirming the reliability of the RNA-seq data.

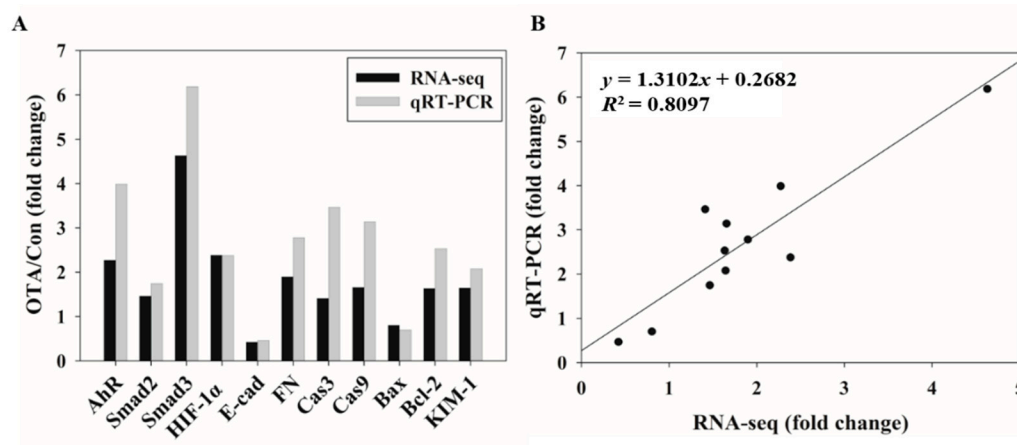


**Figure 4.** Comparison and validation of OTA-induced gene expression changes determined by RNA-seq and qRT-PCR. (A) Fold change of expression value of OTA compared to control measured by RNA-seq and qRT-PCR in eleven selected genes. (B) Correlation plot between RNA-seq fold change (FC) compared to qRT-PCR FC. AhR, Aryl Hydrocarbon Receptor; Smad; HIF-1 $\alpha$ , Hypoxia-inducible factor 1-alpha; E-cad, epithelial-cadherin; FN, Fibronectin; Cas, Caspase; Bax, Bcl-2-associated X protein; Bcl-2, B-cell lymphoma 2; KIM-1, Kidney injury molecule-1.

### 2.5. Effects of AhR Knockdown on EMT and Kidney Injury-Related Marker Expression

We have reported that AhR regulated phase I and II reactions leading to OTA-induced hepatotoxicity [30]. After knockdown of AhR expression in HK-2 kidney cells using siRNA and OTA treatment, mRNA and protein expression was confirmed by qRT-PCR and Western blot analysis, respectively, for markers of EMT, apoptosis, and kidney injury. As shown in Figure 5, E-cad mRNA and protein expression was increased in cells with AhR knockdown. RNA-seq and qPCR data showed that E-cad expression was decreased by OTA treatment in HK-2 cells (Figure 4A). In contrast, FN expression was decreased by the siAhR transfection. The mRNA and protein expression of caspase-3 and Bax, which are pro-apoptotic markers, was suppressed by AhR knockdown. The kidney injury marker, KIM-1, was also suppressed in siAhR-transfected cells.

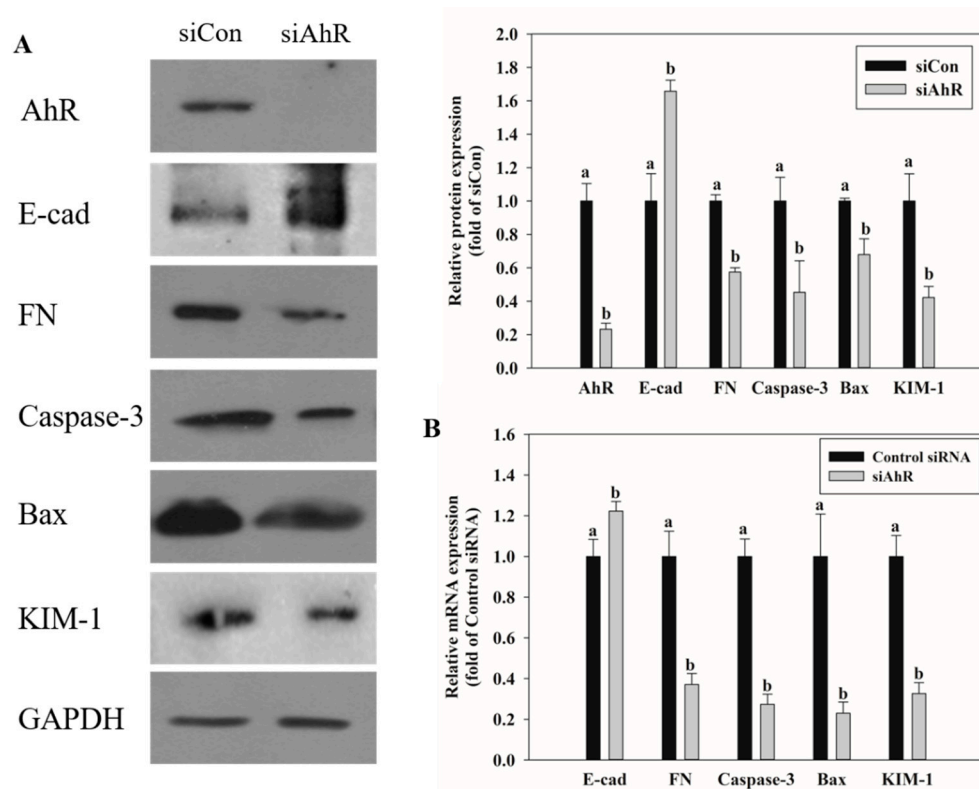


**Figure 5.** Effects of AhR knockdown on EMT, apoptosis, and kidney injury-related markers expression. (A) The protein expression on EMT, apoptosis, and kidney injury-related markers was determined by Western blot after treatment with OTA on HK-2 cells transfected with Control siRNA or siAhR. (B) The mRNA expression on EMT, apoptosis, and kidney injury-related markers was determined by qRT-PCR after treatment with OTA on HK-2 cells transfected with scrambled siRNA (Control siRNA) or AhR-specific siRNA (siAhR). The data are expressed as mean  $\pm$  S.D. values of three independent experiments with three replicate wells. Different letters indicate significant differences compared with control siRNA at  $p < 0.05$  by Tukey's studentized range test.

### 2.6. Effect of AhR Knockdown on Smad2/3 and HIF-1 $\alpha$ Expression

qRT-PCR and Western blot were performed to identify the transcription factors related to EMT and hypoxia upon AhR knockdown in HK-2 cells and treatment with OTA. The expression of Smad2/3, an EMT-related transcription factor, and that of HIF-1 $\alpha$ , a hypoxia-related transcription factor, were also suppressed upon OTA treatment of siAhR-transfected cells (Figure 6).

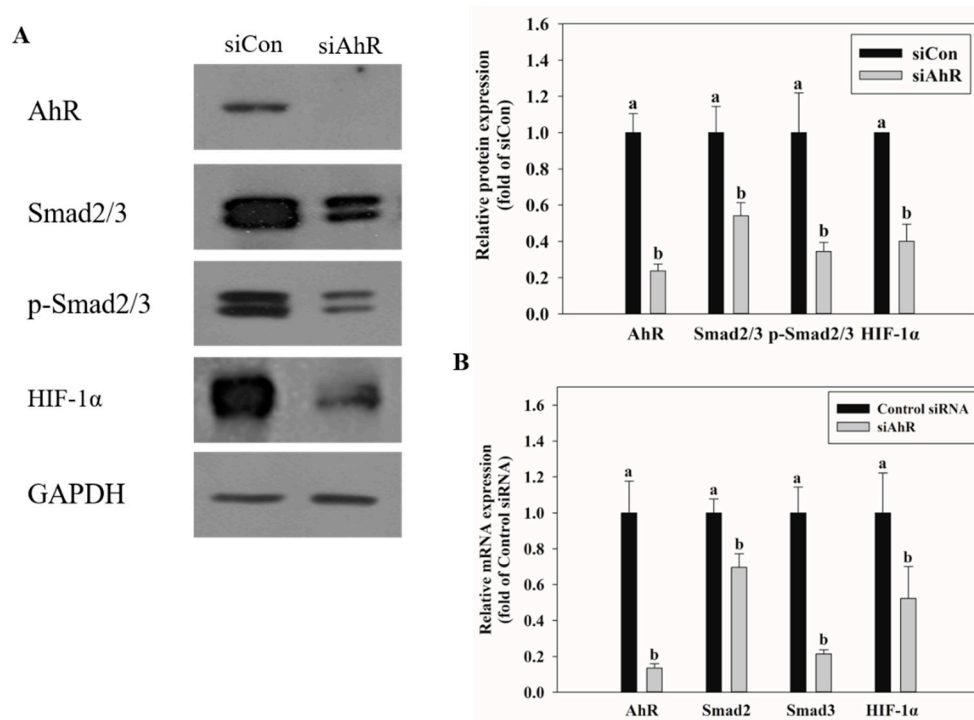


**Figure 6.** Effects of AhR knockdown on Smad2/3 and HIF-1 $\alpha$  expression. **(A)** The protein expression on Smad2/3 and HIF-1 $\alpha$  was determined by Western blot after treatment with OTA on HK-2 cells transfected with Control siRNA or siAhR. **(B)** The mRNA expression on Smad2/3 and HIF-1 $\alpha$  was determined by qRT-PCR after treatment with OTA on HK-2 cells transfected with Control siRNA or siAhR. The data are expressed as mean  $\pm$  S.D. values of three independent experiments with three replicate wells. Different letters indicate significant differences compared with control siRNA at  $p < 0.05$  by Tukey's studentized range test.

### 2.7. Effects of Smad2/3 and HIF-1 $\alpha$ Knockdown on EMT and Renal Injury-Related Markers Expression

To confirm the association between transcription factors Smad2/3 and HIF-1 $\alpha$  and the processes of EMT, apoptosis, and kidney injury caused by OTA treatment, Smad2/3 and HIF-1 $\alpha$  were knocked down with siRNA in HK-2 cells, followed by OTA treatment. The expression of EMT, apoptosis, and kidney injury-related markers was confirmed by qRT-PCR and Western blot. E-cad, which showed decreased expression in OTA treatment, was increased with siSmad2/3 knockdown, whereas siSmad2/3 transfection decreased the expression of FN, caspase-3, Bax, and KIM-1, which were increased by OTA (Figure 7A,B). On the contrary, when HIF-1 $\alpha$  expression was knocked down, E-cad expression was decreased further, and the expression of FN, caspase-3, Bax, and KIM-1 was increased at the mRNA and protein levels (Figure 7).

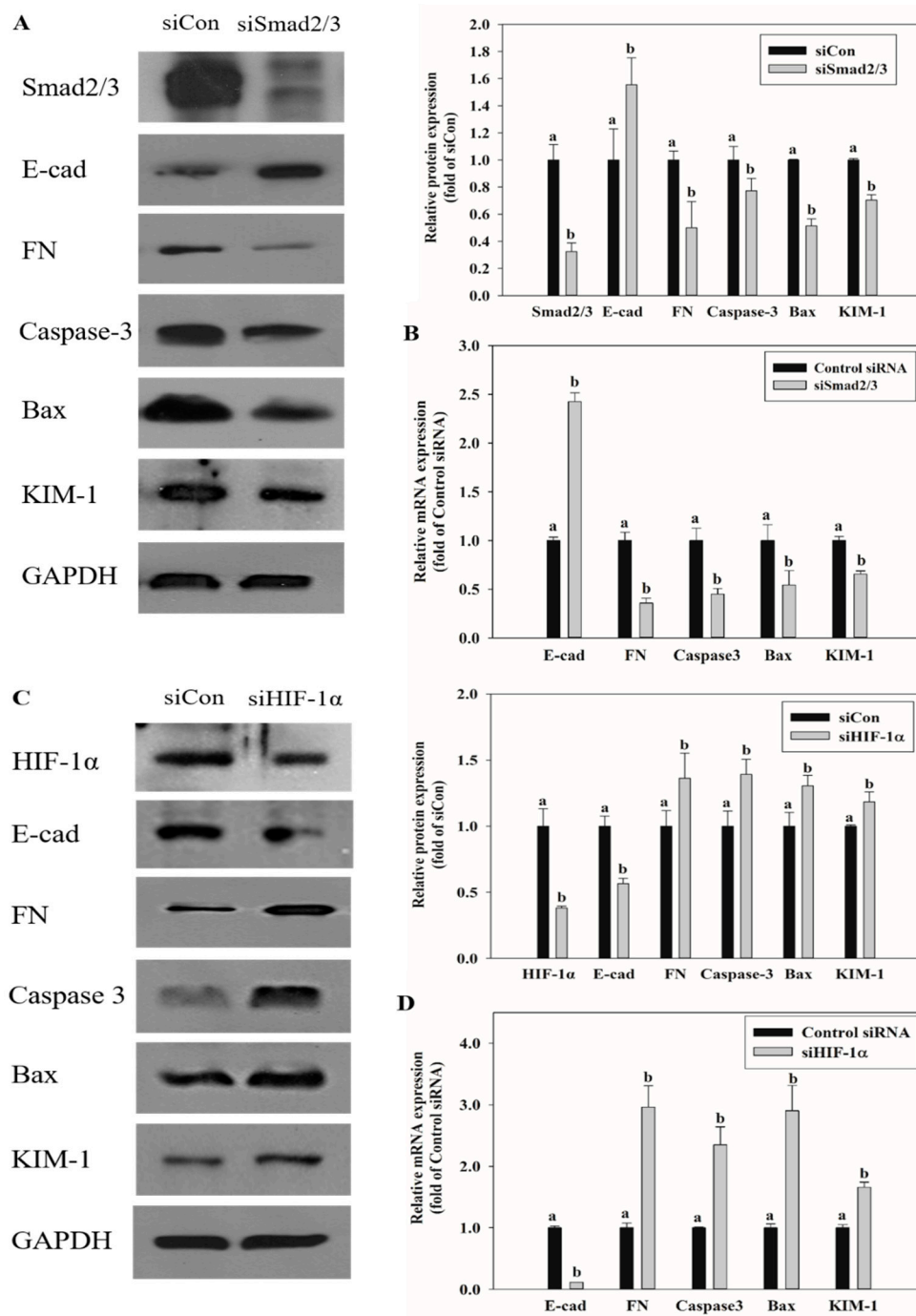


**Figure 7.** Effects of Smad2/3 and HIF-1α knockdown on EMT, apoptosis, and kidney injury-related markers expression. (A) The protein expression on EMT, apoptosis, and kidney injury-related markers was determined by Western blot after treatment with OTA on HK-2 cells transfected with scrambled siRNA (Control siRNA) or Smad2/3-specific siRNA (siSmad2/3). (B) The mRNA expression on EMT, apoptosis, and kidney injury-related markers was determined by qRT-PCR after treatment with OTA on HK-2 cells transfected with Control siRNA or siSmad2/3. (C) The protein expression on EMT, apoptosis, and kidney injury-related markers was determined by Western blot after treatment with OTA on HK-2 cells transfected with scrambled siRNA (Control siRNA) or HIF-1α -specific siRNA (siHIF-1α). (D) The mRNA expression on EMT, apoptosis, and kidney injury-related markers was determined by qRT-PCR after treatment with OTA on HK-2 cells transfected with Control siRNA or siHIF-1α. The data are expressed as mean ± S.D. values of three independent experiments with three replicate wells. Different letters indicate significant differences compared with control siRNA at  $p < 0.05$  by Tukey’s studentized range test.

### 3. Discussion

OTA is a mycotoxin found in various foods that are widely ingested by humans and, owing to its long half-life and thermal stability in food, is highly toxic to humans and animals. It is absorbed through the small intestine after oral intake of OTA [31,32]. In different animal species and in various organs of such animals, OTA toxicity was found [30,33–35]. Research on the mechanism by which OTA causes toxicity, however, is still limited. In this study, by transcriptome analysis using RNA sequencing technique, we attempted to analyze the OTA-regulated pathways and studied the relationship between the pathways and the toxicity of OTA. Transcriptome research, by deciphering the structure and role of the genome, is a tool for studying the pathological processes of disease and offers valuable knowledge on the range of response to pathogens and environmental stress [36]. We focused on hypoxia, xenobiotic metabolism, EMT, and apoptosis, along with the processes that occur in OTA-treated kidney cells, based on previous studies of OTA-induced toxicity pathways [30,37,38] and our transcriptome outcome (Table 1).

Xenobiotic metabolism refers to the metabolic or detoxification processes occurring in the liver and kidneys when toxic substances are biotransformed in the body [39]. Aflatoxin A or benzo(a)pyrene are activated by xenobiotic metabolism [40,41]. During xenobiotic metabolism, a transcription factor called AhR, which regulates the expression of cytochrome P450 (CYP) enzymes is activated. Subsequent activation of AhR might produce oxidative stress and ROS, resulting in cancer induction and immune function suppression [42,43]. Our previous *in vitro* and *in vivo* study using HK-2 cells and ICR male mice reported significantly increased mRNA and protein expression of CYP1A1 and CYP1A2 in the group treated with OTA compared to the control group, and when HK-2 cells were exposed to OTA, AhR-activated renal damage was caused by excessive ROS production during the metabolic processes involving CYP enzymes [35]. Generation of excessive oxidative stress also causes apoptosis and EMT [44,45].

Apoptosis occurs through two pathways, the intrinsic and extrinsic apoptotic pathways, both of which induce the caspase cascade [46]. Apoptosis is considered an important process in cell cell death [47]. Several studies have documented the induction of cellular apoptosis via oxidative stress upon OTA exposure [48,49]. Based on our RNA-seq and qRT-PCR results in HK-2 cells, the expression of Bax and caspase-3 was reduced after knocking down the expression of AhR indicating that OTA-induced apoptosis is triggered via AhR (Figure 5).

EMT is an important event in tumor metastasis where epithelial cells lose their epithelial function and cell–cell adhesion to acquire the mobility and invasive features of mesenchymal cells [50]. This transformation leads to loss of cell junctions and separation between cells and the basement membrane, resulting in cancer stem cell-like properties [51]. Further, instability of adherens junction due to downregulation of E-cadherin in epithelial cells and upregulation of fibronectin in mesenchymal cells are the representative features of EMT [52]. Many studies have shown that EMT progresses by the activation of AhR [53,54]. In this experiment, downregulation of E-cad and upregulation of FN with OTA treatment were confirmed through RNA-seq and qRT-PCR, and OTA was found to induce EMT (Figure 4). Upon OTA treatment after suppressing AhR expression, Smad2/3, an EMT-induced transcription factor, was suppressed (Figure 6) with E-cad upregulation and FN downregulation, which are regulated by Smad2/3 (Figure 5). These results indicate that OTA induces EMT through the AhR-Smad2/3 pathway. Further, studies have shown that apoptosis is induced in the liver and kidney through the Smad3 pathway [55,56]. Smad2/3 expression was suppressed to validate the association between EMT and apoptosis, and caspase-3, Bax, and KIM-1 expressions were decreased on OTA treatment. These results showed that like EMT, OTA induces apoptosis and kidney injury through the AhR-Smad2/3 pathway (Figure 7).

Hypoxia is a condition in which the oxygen supply in cells and organs is insufficient. It is expected to occur in kidney tissues due to microcirculation disruption and

hypoperfusion [57]. In various clinical and laboratory settings, hypoxia is also reported to occur in both acute kidney injury and chronic kidney disease [58,59]. The role of HIF-1 $\alpha$  in hypoxia-induced apoptosis is controversial, but some studies have shown that under particular conditions, HIF-1 $\alpha$  protects cells against apoptosis [60–62]. It is also known that HIF-1 $\alpha$  protects cells against hypoxic kidney damage by upregulating cell-protective factors such as VEGF, HO-1, and erythropoietin [63–65]. Moreover, studies in rat models of renal ischemia/reperfusion have shown that chemical damage is increased when HIF-1 $\alpha$  is inhibited, while accumulation of HIF-1 $\alpha$  has a protective effect against damage [66,67]. It is known that EMT and fibrosis progress after renal ischemia-reperfusion injury [57] [57,68]. HIF-1 $\alpha$  plays a protective role against IRI in the kidney [67]. It protects against IRI by decreasing renal IRI-induced expression of fibrosis and alpha-SMA through increasing HIF- $\alpha$  levels [69]. In this study, the HIF-1 $\alpha$  expression in HK-2 cells was knocked down using siRNA. The expression of Bax, caspase-3, KIM-1, and FN was found to be increased, whereas E-cad decreased. These results show that HIF-1 $\alpha$  is stabilized due to an adaptive response to OTA-induced hypoxia and serves to suppress the progression of apoptosis, EMT, and kidney injury (Figure 7).

In conclusion, EMT and apoptosis in the kidney are triggered by OTA and effectively lead to kidney injury. In addition, EMT, apoptosis, and kidney damage caused by OTA can occur in association with the AhR-Smad2/3-HIF-1 $\alpha$  pathways. Thus, our findings can contribute to understanding the mechanism and prevention of renal toxicity of OTA, such as OTA-induced EMT and apoptosis.

## 4. Materials and Methods

### 4.1. Chemicals

Fetal bovine serum (FBS) and Roswell Park Memorial Institute (RPMI) 1640 medium were purchased from Gibco (Grand Island, NY, USA). Penicillin-streptomycin and trypsin-ethylenediaminetetraacetic acid (EDTA) were purchased from Hyclone (Logan, UT, USA). Dextrose, sodium bicarbonate, 4-(2-Hydroxyethyl) piperazine-1-ethanesulfonic acid (HEPES), dimethyl sulfoxide (DMSO), and thiazolyl blue tetrazolium bromide (MTT) were purchased from Sigma-Aldrich (St. Louis, MO, USA). Bicinchoninic acid (BCA) kit and SuperSignal™ west Femto chemiluminescent substrate were purchased from Thermo Fisher Scientific (Waltham, MA, USA). Antibodies against Smad2/3 and kidney injury molecule-1 (KIM-1) were purchased from Cell Signaling (Denver, MA, USA). Glyceraldehyde-3-phosphate dehydrogenase (GAPDH) antibody was obtained from Millipore (Temecula, CA, USA). Antibodies against AhR, hypoxia-inducible factor 1-alpha (HIF-1 $\alpha$ ), epithelial cadherin (E-cad), fibronectin (FN), and Bcl-2-associated X protein (Bax), caspase-3 were purchased from Santa Cruz Biotechnology (Dallas, TX, USA). AhR siRNA (5'-GUGACUUGUACAGCAUAAUTT-3') was purchased from GenePharma (Shanghai, China), Smad2/3 siRNA (sc-37238) was purchased from Santa Cruz Biotechnology (Santa Cruz, CA, USA), and HIF-1 $\alpha$  siRNA (SASI\_HS02\_00332063) was purchased from Sigma-Aldrich (St. Louis, MO, USA).

### 4.2. Cell Culture

HK-2, a human-derived proximal tubule epithelial cell line, was purchased from Korea Cell Line Bank (Seoul, Korea). HK-2 cells were cultured in RPMI 1640 medium containing 0.11 g/L sodium pyruvate, 2.5 g/L dextrose, 2.383 g/L HEPES, 100 U/mL penicillin, and streptomycin, 2 g/L sodium bicarbonate, and 10% FBS (*v/v*), in an incubator at 37 °C with 5% CO<sub>2</sub>. Cells were cultured until the cell density reached 80–90%.

### 4.3. OTA Treatment of HK-2 Cells

OTA (purity: 99%, Cfm Oskar Tropitzsch GmbH, Marktredwitz, Germany) was dissolved in DMSO at a concentration of 200  $\mu$ M and stored at –20 °C until used in experiments. In the experiments, to prepare 200 nM OTA, it was diluted into RPMI1640 media. In both the OTA treated group and the non-OTA treated control group, the final DMSO

concentration was 0.1%. In our previous studies, exposure to 200 nM OTA induced kidney and liver toxicity [30,35]. Therefore, in this study, we used 200 nM OTA in HK-2 cells for 48 h to identify the mechanism of toxicity.

#### 4.4. Cytotoxicity Assay

HK-2 cells were seeded at  $1 \times 10^5$  cells/well in a 24 well polystyrene plate (Falcon, Corning, NY, USA). Cell viability was confirmed using the MTT assay [70]. After 24 h of seeding, the cells were treated with OTA for 48 h. After that, the treated medium was removed, 200  $\mu$ L of MTT solution (1 mg/mL) was added, and incubated for 4 h. Then, 100  $\mu$ L of DMSO was added after removing the MTT solution to dissolve the formazan crystals formed in living cells. Then, the DMSO with dissolved formazan was transferred to a 96-well plate at 50  $\mu$ L per well, and its absorbance at 540 nm was measured using a multiplate reader (EL-808, BioTek, Winooski, VT, USA). Three independent experiments ( $n = 3$ ) with three replicate wells were performed.

#### 4.5. Total RNA Isolation and Quantitative Real-Time PCR (qRT-PCR)

To examine mRNA expression, the treated HK-2 cells were washed twice with ice-cold PBS, and RNAiso Plus (Takara, Kusatu, Japan) was added to isolate the total RNA. The total RNA concentration in each sample was determined by a Nanodrop 1000 spectrophotometer (Thermo Fisher Scientific, Waltham, MA, USA). Only samples with a Nanodrop A260:280 ratio between 1.8 and 2.1 were used in the experiment. cDNA was synthesized using 2  $\mu$ g of total RNA and the cocktail solution according to the manufacturer's instruction in the cDNA synthesis kit (Legene Biosciences, San Diego, CA, USA). In order to confirm the cDNA quality,  $\beta$ -actin, a house keeping gene, was confirmed in agarose gel, and it was also confirmed that the Ct value appeared at a level of 23 to 25 in qRT-PCR. The sequences of primers used in this experiment are shown in Table S1. Primers were checked by using the NCBI tool Primer-Blast (<https://www.ncbi.nlm.nih.gov/tools/primer-blast/>, accessed on 10 January 2021). qRT-PCR was performed using 0.5  $\mu$ L of cDNA, 9.5  $\mu$ L of primer cocktail, and 10  $\mu$ L of SYBR green in a total reaction volume of 20  $\mu$ L on the BioRad iQ5 thermal cycler according to the manufacturer's protocols (iQ SYBR Green Supermix, Bio-Rad, Hercules, CA, USA). The results were analyzed using the comparative Ct method as described previously [35]. The comparative Ct method was used for relative quantification and normalized using a housekeeping gene ( $\beta$ -actin) and expressed as  $2^{-\Delta\Delta Ct}$  values.

#### 4.6. Isolation of Total Cell Lysate and Western Blot Analysis

To isolate total cell lysate, HK-2 cells were lysed using RIPA buffer (25 mM Tris-Cl pH 7.4, 1% Triton X-100, 0.1% SDS, 0.5% deoxycholic acid, 10% glycerol, 150 mM NaCl, 5 mM EDTA, 1 mM PMSF, 5  $\mu$ g/mL aprotinin, leupeptin and phosphatase inhibitor). The lysed cells were incubated on ice for 30 min and centrifuged at 13,000 rpm and 4  $^{\circ}$ C for 20 min. The resulting supernatant was used as a total cell lysate. Proteins were separated on 7.5–15% SDS-polyacrylamide gels and electrotransferred to PVDF membranes. The transferred membrane was blocked using 5% skim milk, and immunoblotting was performed using monoclonal AhR (1:200), Smad2/3 (1:1000), p-Smad2/3 (1:1000), HIF-1 $\alpha$  (1:200), E-cad (1:1000), FN (1:200), caspase-3 (1:200), Bax (1:200), KIM-1 (1:1000), and GAPDH (1:4000), and then incubated with peroxidase-conjugated secondary antibodies (1:4000). Protein bands were detected using SuperSignal<sup>TM</sup> West Femto. The intensity of the bands was quantified using Image J program (National Institutes of Health, Maryland, USA), and the protein expressions were normalized to the levels of GAPDH. The control group was set to 1 and the other group was compared with the control group.

#### 4.7. Transfection with Small Interfering RNA (siRNA)

HK-2 cells ( $2 \times 10^5$  cells/well in 6 well plate) were transfected with AhR, Smad2/3 and HIF-1 $\alpha$ -specific siRNA using Lipofectamine<sup>TM</sup> RNAiMAX transfection reagent (Invitrogen, Carlsbad, CA, USA) by the reverse transfection method as per the manufacturer's

protocol. Briefly, after transfection with 100 pmol siRNA in 500  $\mu$ L of Opti-MEM and 5  $\mu$ L Lipofectamine<sup>TM</sup> RNAiMAX for 48 h, cells were treated with 200 nM OTA for 48 h and then isolated for experimental purposes such as qRT-PCR or Western blot. The transfection was repeated 3 times for each siRNA.

#### 4.8. RNA-sequencing

The quality of RNA used for RNA-sequencing was evaluated by Agilent 2100 bioanalyzer using the RNA 6000 Nano Chip (Agilent Technologies, Amstelveen, Netherlands), and RNA quantification was performed using ND-2000 Spectrophotometer (Thermo Inc., DE, USA).

An Ion AmpliSeq<sup>TM</sup> Transcriptome library was constructed with the Ion Transcriptome Human Gene Expression Kit (Thermo Fisher Scientific, Waltham, MA, USA) as manufacturer's instruction, and as published [71]. 50 ng of total RNA were reverse transcribed to make cDNA by random priming. cDNA product was amplified target genes using the Ion AmpliSeq Transcriptome Human Gene Expression Core Panel with the Ion AmpliSeq<sup>TM</sup> Library Kit which is designed for the targeted amplification of more than 20,000 human RefSeq genes simultaneously in a single primer pool. Short amplicons (~100 base pairs (bp)) for the target genes are amplified. After primer digestion, adapters and molecular barcodes were ligated to the amplicons followed by magnetic bead purification. This library concentration were measured using Ion Library Quantitation Kit (Thermo Fisher Scientific, Waltham, MA, USA) according to the manufacturer's recommendation. Multiple libraries were multiplexed and clonally amplified using the Ion Chef System, and were sequenced on the Ion Torrent S5XL machine (Thermo Fisher Scientific, Waltham, MA, USA).

#### 4.9. RNA-seq Data Analysis

All sequencing data was processed on Ion S5xl Sequencer (Thermo Fisher Scientific, Waltham, MA, USA) and transferred to the Ion Proton<sup>TM</sup> Torrent Server for primary data analysis with gene-level transcript quantification from sequence read data performed using AmpliSeq RNA Plug in (ver 5.6.0.3) by Torrent Suite Software (Thermo Fisher Scientific, Waltham, MA, USA). Identification of up or down-regulated genes was performed using the Excel-based Differentially Expressed Gene Analysis software (ExDEGA version 1.6.3, e-Biogen, Seoul, Korea). The DEG list was filtered using a 5% false discovery rate (FDR) cutoff and  $|\text{Fold change (FC)}| > 2.0$  for upregulated and downregulated genes. Gene ontology (GO) and Kyoto Encyclopedia of Genes and Genomes (KEGG, Kyoto, Japan) Pathway Enrichment analysis for OTA was executed using the database for annotation, visualization, and integrated discovery (DAVID, Frederick, MA, USA) version 6.8 (<https://david.ncicrf.gov>, accessed on 10 January 2021) functional annotation system [72]. The gene set enrichment analysis (GSEA; Broad Institute) software platform (MSigDB version 6.1, Massachusetts, CA, USA) was used to identify different expression pathways from control cells in OTA-treated cells by comparing them with hallmark gene sets representing specific well-defined biological states [73].

#### 4.10. Statistical Analysis of Experiments

All experimental values were expressed as the mean  $\pm$  standard deviation. Statistically significant differences between groups were calculated using Kruskal–Wallis test and non-parametric Mann–Whitney *U*-test for non-normal distributed data. All statistical analyses were performed in IBM SPSS Statistics version 24 (IBM, Armonk, NY, USA). Different letters indicate significant differences at  $p < 0.05$ . The data are expressed as mean  $\pm$  S.D. values of three independent experiments ( $n = 3$ ) with three replicates.

**Supplementary Materials:** The following are available online at <https://www.mdpi.com/2072-6651/13/3/190/s1>, Table S1: Human qPCR primer sequences used in the experiments.

**Author Contributions:** Study concept and design, M.C.P. and K.-W.L.; Analysis and interpretation of data, M.C.P., I.-G.C. and K.-W.L.; Drafting of the manuscript, M.C.P. and K.-W.L.; Final approval of the manuscript, K.-W.L. All authors have read and agreed to the published version of the manuscript.

**Funding:** This research was supported by National Research Foundation of Korea (NRF) grant funded by the Korea government (MIST) (No. 2021R1A2C1007428) and Korea University Grant (K1803651) of School of Life Sciences, South Korea.

**Institutional Review Board Statement:** Not applicable

**Informed Consent Statement:** Not applicable

**Data Availability Statement:** The data presented in this study are available in article or supplementary materials here.

**Acknowledgments:** This research was supported by School of Life Sciences & Biotechnology of Korea University for BK21PLUS, South Korea. The authors thank the Institute of Biomedical Science & Food Safety, CJ-Korea University Food Safety Hall (Seoul, South Korea) for providing the equipment and facilities.

**Conflicts of Interest:** The authors declare no conflict of interest

## References

1. Liang, Z.; Huang, K.; Luo, Y. Ochratoxin A and ochratoxin-producing fungi on cereal grain in China: A review. *Food Addit. Contam. Part A* **2015**, *32*, 461–470.
2. Bui-Klimke, T.R.; Wu, F. Ochratoxin A and human health risk: A review of the evidence. *Crit. Rev. Food Sci. Nutr.* **2015**, *55*, 1860–1869. [[CrossRef](#)] [[PubMed](#)]
3. Van der Merwe, K.; Steyn, P.; Fourie, L.; Scott, D.B.; Theron, J. Ochratoxin A, a toxic metabolite produced by *Aspergillus ochraceus* Wilh. *Nature* **1965**, *205*, 1112–1113. [[CrossRef](#)] [[PubMed](#)]
4. Delacruz, L.; Bach, P. The role of ochratoxin A metabolism and biochemistry in animal and human nephrotoxicity. *J. Biopharm. Sci.* **1990**, *1*, 277–304.
5. Galtier, P.; Alvinerie, M.; Charpentreau, J. The pharmacokinetic profiles of ochratoxin A in pigs, rabbits and chickens. *Food Cosmet. Toxicol.* **1981**, *19*, 735–738. [[CrossRef](#)]
6. IARC. *Some Naturally Occurring Substances: Food Items and Constituents, Heterocyclic Aromatic Amines and Mycotoxins*; IARC Monographs on the Evaluation of the Carcinogenic Risk of Chemicals to Humans; World Health Organization: Geneva, Switzerland, 1993; Volume 56.
7. Pfohl-Leszkowicz, A.; Manderville, R.A. Ochratoxin A: An overview on toxicity and carcinogenicity in animals and humans. *Mol. Nutr. Food Res.* **2007**, *51*, 61–99. [[CrossRef](#)] [[PubMed](#)]
8. Mally, A.; Dekant, W. Mycotoxins and the kidney: Modes of action for renal tumor formation by ochratoxin A in rodents. *Mol. Nutr. Food Res.* **2009**, *53*, 467–478. [[CrossRef](#)] [[PubMed](#)]
9. Gan, F.; Hou, L.; Zhou, Y.; Liu, Y.; Huang, D.; Chen, X.; Huang, K. Effects of ochratoxin A on ER stress, MAPK signaling pathway and autophagy of kidney and spleen in pigs. *Environ. Toxicol.* **2017**, *32*, 2277–2286. [[CrossRef](#)]
10. Damiano, S.; Iovane, V.; Squillacioti, C.; Mirabella, N.; Prisco, F.; Ariano, A.; Amenta, M.; Giordano, A.; Florio, S.; Ciarcia, R. Red orange and lemon extract prevents the renal toxicity induced by ochratoxin A in rats. *J. Cell. Physiol.* **2020**, *235*, 5386–5393. [[CrossRef](#)]
11. Damiano, S.; Longobardi, C.; Andretta, E.; Prisco, F.; Piegari, G.; Squillacioti, C.; Montagnaro, S.; Pagnini, F.; Badino, P.; Florio, S. Antioxidative Effects of Curcumin on the Hepatotoxicity Induced by Ochratoxin A in Rats. *Antioxidants* **2021**, *10*, 125. [[CrossRef](#)]
12. Cui, G.; Li, L.; Xu, W.; Wang, M.; Jiao, D.; Yao, B.; Xu, K.; Chen, Y.; Yang, S.; Long, M. Astaxanthin protects ochratoxin A-induced oxidative stress and apoptosis in the heart via the Nrf2 pathway. *Oxidative Med. Cell. Longev.* **2020**. [[CrossRef](#)] [[PubMed](#)]
13. Zhou, Q.; Chen, W.; Yu, X.-Q. Long non-coding RNAs as novel diagnostic and therapeutic targets in kidney disease. *Chronic Dis. Transl. Med.* **2020**. [[CrossRef](#)] [[PubMed](#)]
14. Han, X.; Shi, Y.; Diamond-Stanic, M.; Sharma, K. Role of Mitochondria in the Regulation of Kidney Function and Metabolism in Type 2 Diabetes. In *Mitochondria in Obesity and Type 2 Diabetes*; Elsevier: Amsterdam, The Netherlands, 2019; pp. 287–300.
15. Radford, R.; Frain, H.; Ryan, M.P.; Slattery, C.; McMorrow, T. Mechanisms of chemical carcinogenesis in the kidneys. *Int. J. Mol. Sci.* **2013**, *14*, 19416–19433. [[CrossRef](#)]
16. Zingerle, M.; Silbernagl, S.; Gekle, M. Reabsorption of the nephrotoxin ochratoxin A along the rat nephron in vivo. *J. Pharmacol. Exp. Ther.* **1997**, *280*, 220–224.
17. Schwerdt, G.; Bauer, K.; Gekle, M.; Silbernagl, S. Accumulation of ochratoxin A in rat kidney in vivo and in cultivated renal epithelial cells in vitro. *Toxicology* **1996**, *114*, 177–185. [[CrossRef](#)]
18. Kashida, Y.; Takahashi, A.; Moto, M.; Okamura, M.; Muguruma, M.; Jin, M.; Arai, K.; Mitsumori, K. Gene expression analysis in mice liver on hepatocarcinogenesis by flumequine. *Arch. Toxicol.* **2006**, *80*, 533–539. [[CrossRef](#)] [[PubMed](#)]

19. Zheng, M.; Lu, J.; Zhao, D. Toxicity and transcriptome sequencing (RNA-seq) analyses of adult zebrafish in response to exposure carboxymethyl cellulose stabilized iron sulfide nanoparticles. *Sci. Rep.* **2018**, *8*, 1–11. [[CrossRef](#)] [[PubMed](#)]
20. Chen, M.; Zhang, M.; Borlak, J.; Tong, W. A decade of toxicogenomic research and its contribution to toxicological science. *Toxicol. Sci.* **2012**, *130*, 217–228. [[CrossRef](#)] [[PubMed](#)]
21. Wentzel, J.F.; Lombard, M.J.; Du Plessis, L.H.; Zandberg, L. Evaluation of the cytotoxic properties, gene expression profiles and secondary signalling responses of cultured cells exposed to fumonisin B1, deoxynivalenol and zearalenone mycotoxins. *Arch. Toxicol.* **2017**, *91*, 2265–2282. [[CrossRef](#)]
22. Afshari, C.A.; Hamadeh, H.K.; Bushel, P.R. The evolution of bioinformatics in toxicology: Advancing toxicogenomics. *Toxicol. Sci.* **2011**, *120*, S225–S237. [[CrossRef](#)]
23. Arbillaga, L.; Azqueta, A.; van Delft, J.H.; de Cerain, A.L. In vitro gene expression data supporting a DNA non-reactive genotoxic mechanism for ochratoxin A. *Toxicol. Appl. Pharmacol.* **2007**, *220*, 216–224. [[CrossRef](#)]
24. Hibi, D.; Kijima, A.; Kuroda, K.; Suzuki, Y.; Ishii, Y.; Jin, M.; Nakajima, M.; Sugita-Konishi, Y.; Yanai, T.; Nohmi, T. Molecular mechanisms underlying ochratoxin A-induced genotoxicity: Global gene expression analysis suggests induction of DNA double-strand breaks and cell cycle progression. *J. Toxicol. Sci.* **2013**, *38*, 57–69. [[CrossRef](#)] [[PubMed](#)]
25. Hundhausen, C.; Boesch-Saadatmandi, C.; Matzner, N.; Lang, F.; Blank, R.; Wolffram, S.; Blaschek, W.; Rimbach, G. Ochratoxin A lowers mRNA levels of genes encoding for key proteins of liver cell metabolism. *Cancer Genom. Proteom.* **2008**, *5*, 319–332.
26. Raghubeer, S.; Nagiah, S.; Chaturgoon, A.A. Acute Ochratoxin A exposure induces inflammation and apoptosis in human embryonic kidney (HEK293) cells. *Toxicol.* **2017**, *137*, 48–53. [[CrossRef](#)] [[PubMed](#)]
27. Li, H.; Mao, X.; Liu, K.; Sun, J.; Li, B.; Malyar, R.M.; Liu, D.; Pan, C.; Gan, F.; Liu, Y. Ochratoxin A induces nephrotoxicity in vitro and in vivo via pyroptosis. *Arch. Toxicol.* **2021**. [[CrossRef](#)] [[PubMed](#)]
28. Jiang, J.; Tang, Y.-L.; Liang, X.-H. EMT: A new vision of hypoxia promoting cancer progression. *Cancer Biol. Ther.* **2011**, *11*, 714–723. [[CrossRef](#)]
29. Myszczyzyn, A.; Czarnecka, A.M.; Matak, D.; Szymanski, L.; Lian, F.; Kornakiewicz, A.; Bartnik, E.; Kukwa, W.; Kieda, C.; Szczylik, C. The role of hypoxia and cancer stem cells in renal cell carcinoma pathogenesis. *Stem Cell Rev. Rep.* **2015**, *11*, 919–943. [[CrossRef](#)] [[PubMed](#)]
30. Shin, H.S.; Lee, H.J.; Pyo, M.C.; Ryu, D.; Lee, K.-W. Ochratoxin A-Induced Hepatotoxicity through Phase I and Phase II Reactions Regulated by AhR in Liver Cells. *Toxins* **2019**, *11*, 377. [[CrossRef](#)] [[PubMed](#)]
31. Peraica, M.; Flajs, D.; Domijan, A.-M.; Ivić, D.; Cvjetković, B. Ochratoxin A contamination of food from Croatia. *Toxins* **2010**, *2*, 2098–2105. [[CrossRef](#)]
32. Sergent, T.; Garsou, S.; Schaut, A.; De Saeger, S.; Pussemier, L.; Van Peteghem, C.; Larondelle, Y.; Schneider, Y.-J. Differential modulation of ochratoxin A absorption across Caco-2 cells by dietary polyphenols, used at realistic intestinal concentrations. *Toxicol. Lett.* **2005**, *159*, 60–70. [[CrossRef](#)] [[PubMed](#)]
33. Yang, X.; Xu, W.; Huang, K.; Zhang, B.; Wang, H.; Zhang, X.; Gong, L.; Luo, Y.; He, X. Precision toxicology shows that troxerutin alleviates ochratoxin A-induced renal lipotoxicity. *FASEB J.* **2019**, *33*, 2212–2227. [[CrossRef](#)] [[PubMed](#)]
34. Zhu, L.; Yu, T.; Qi, X.; Gao, J.; Huang, K.; He, X.; Luo, H.; Xu, W. Limited link between oxidative stress and ochratoxin A—Induced renal injury in an acute toxicity rat model. *Toxins* **2016**, *8*, 373. [[CrossRef](#)] [[PubMed](#)]
35. Lee, H.J.; Pyo, M.C.; Shin, H.S.; Ryu, D.; Lee, K.-W. Renal toxicity through AhR, PXR, and Nrf2 signaling pathway activation of ochratoxin A-induced oxidative stress in kidney cells. *Food Chem. Toxicol.* **2018**, *122*, 59–68. [[CrossRef](#)]
36. Jiang, Z.; Zhou, X.; Li, R.; Michal, J.J.; Zhang, S.; Dodson, M.V.; Zhang, Z.; Harland, R.M. Whole transcriptome analysis with sequencing: Methods, challenges and potential solutions. *Cell. Mol. Life Sci.* **2015**, *72*, 3425–3439. [[CrossRef](#)] [[PubMed](#)]
37. Raghubeer, S.; Nagiah, S.; Chaturgoon, A. Ochratoxin A upregulates biomarkers associated with hypoxia and transformation in human kidney cells. *Toxicol. In Vitro* **2019**, *57*, 211–216. [[CrossRef](#)] [[PubMed](#)]
38. Schwerdt, G.; Holzinger, H.; Sauvant, C.; Königs, M.; Humpf, H.-U.; Gekle, M. Long-term effects of ochratoxin A on fibrosis and cell death in human proximal tubule or fibroblast cells in primary culture. *Toxicology* **2007**, *232*, 57–67. [[CrossRef](#)]
39. Hodges, R.E.; Minich, D.M. Modulation of metabolic detoxification pathways using foods and food-derived components: A scientific review with clinical application. *J. Nutr. Metab.* **2015**. [[CrossRef](#)] [[PubMed](#)]
40. Lu, Y.; Cederbaum, A.I. CYP2E1 potentiation of LPS and TNF $\alpha$ -induced hepatotoxicity by mechanisms involving enhanced oxidative and nitrosative stress, activation of MAP kinases, and mitochondrial dysfunction. *Genes Nutr.* **2010**, *5*, 149–167. [[CrossRef](#)] [[PubMed](#)]
41. Vázquez-Gómez, G.; Rocha-Zavaleta, L.; Rodríguez-Sosa, M.; Petrosyan, P.; Rubio-Lightbourn, J. Benzo [a] pyrene activates an AhR/Src/ERK axis that contributes to CYP1A1 induction and stable DNA adducts formation in lung cells. *Toxicol. Lett.* **2018**, *289*, 54–62. [[CrossRef](#)] [[PubMed](#)]
42. Nebert, D.W. Aryl hydrocarbon receptor (AHR): “pioneer member” of the basic-helix/loop/helix per-Arnt-sim (bHLH/PAS) family of “sensors” of foreign and endogenous signals. *Prog. Lipid Res.* **2017**, *67*, 38–57. [[CrossRef](#)] [[PubMed](#)]
43. Phillips, T.D.; Richardson, M.; Cheng, Y.-S.L.; He, L.; McDonald, T.J.; Cizmas, L.H.; Safe, S.H.; Donnelly, K.C.; Wang, F.; Moorthy, B. Mechanistic relationships between hepatic genotoxicity and carcinogenicity in male B6C3F1 mice treated with polycyclic aromatic hydrocarbon mixtures. *Arch. Toxicol.* **2015**, *89*, 967–977. [[CrossRef](#)] [[PubMed](#)]
44. Li, Y.; Yang, M.; Meng, T.; Niu, Y.; Dai, Y.; Zhang, L.; Zheng, X.; Jalava, P.; Dong, G.; Gao, W. Oxidative stress induced by ultrafine carbon black particles can elicit apoptosis in vivo and vitro. *Sci. Total Environ.* **2020**, *709*, 135802. [[CrossRef](#)] [[PubMed](#)]

45. Tang, Z.; Chen, H.; He, H.; Ma, C. Assays for alkaline phosphatase activity: Progress and prospects. *Trac Trends Anal. Chem.* **2019**. [[CrossRef](#)]
46. Kroemer, G.; Galluzzi, L.; Brenner, C. Mitochondrial membrane permeabilization in cell death. *Physiol. Rev.* **2007**, *87*, 99–163. [[CrossRef](#)]
47. Elmore, S. Apoptosis: A review of programmed cell death. *Toxicol. Pathol.* **2007**, *35*, 495–516. [[CrossRef](#)]
48. Petrik, J.; Žanić-Grubišić, T.; Barišić, K.; Pepeljnjak, S.; Radić, B.; Ferenčić, Ž.; Čepelak, I. Apoptosis and oxidative stress induced by ochratoxin A in rat kidney. *Arch. Toxicol.* **2003**, *77*, 685–693. [[CrossRef](#)] [[PubMed](#)]
49. Ramyaa, P.; Padma, V.V. Ochratoxin-induced toxicity, oxidative stress and apoptosis ameliorated by quercetin—Modulation by Nrf2. *Food Chem. Toxicol.* **2013**, *62*, 205–216. [[CrossRef](#)]
50. Bartis, D.; Mise, N.; Mahida, R.Y.; Eickelberg, O.; Thickett, D.R. Epithelial–mesenchymal transition in lung development and disease: Does it exist and is it important? *Thorax* **2014**, *69*, 760–765. [[CrossRef](#)]
51. Dongre, A.; Weinberg, R.A. New insights into the mechanisms of epithelial–mesenchymal transition and implications for cancer. *Nat. Rev. Mol. Cell Biol.* **2019**, *20*, 69–84. [[CrossRef](#)] [[PubMed](#)]
52. Benzoubir, N.; Mussini, C.; Lejamtel, C.; Dos Santos, A.; Guillaume, C.; Desterke, C.; Samuel, D.; Brechot, C.; Bourgeade, M.-F.; Guettier, C. Gamma-smooth muscle actin expression is associated with epithelial–mesenchymal transition and stem-like properties in hepatocellular carcinoma. *PLoS ONE* **2015**, *10*, e0130559. [[CrossRef](#)] [[PubMed](#)]
53. Gao, Z.; Bu, Y.; Liu, X.; Wang, X.; Zhang, G.; Wang, E.; Ding, S.; Liu, Y.; Shi, R.; Li, Q. TCDD promoted EMT of hFPCEs via AhR, which involved the activation of EGFR/ERK signaling. *Toxicol. Appl. Pharmacol.* **2016**, *298*, 48–55. [[CrossRef](#)]
54. Wu, Y.; Niu, Y.; Leng, J.; Xu, J.; Chen, H.; Li, H.; Wang, L.; Hu, J.; Xia, D.; Wu, Y. Benzo (a) pyrene regulated A549 cell migration, invasion and epithelial–mesenchymal transition by up-regulating long non-coding RNA linc00673. *Toxicol. Lett.* **2020**, *320*, 37–45. [[CrossRef](#)] [[PubMed](#)]
55. Inazaki, K.; Kanamaru, Y.; Kojima, Y.; Sueyoshi, N.; Okumura, K.; Kaneko, K.; Yamashiro, Y.; Ogawa, H.; Nakao, A. Smad3 deficiency attenuates renal fibrosis, inflammation, and apoptosis after unilateral ureteral obstruction. *Kidney Int.* **2004**, *66*, 597–604. [[CrossRef](#)] [[PubMed](#)]
56. Black, D.; Lyman, S.; Qian, T.; Lemasters, J.J.; Rippe, R.A.; Nitta, T.; Kim, J.-S.; Behrns, K.E. Transforming growth factor beta mediates hepatocyte apoptosis through Smad3 generation of reactive oxygen species. *Biochimie* **2007**, *89*, 1464–1473. [[CrossRef](#)] [[PubMed](#)]
57. Matsumoto, M.; Tanaka, T.; Yamamoto, T.; Noiri, E.; Miyata, T.; Inagi, R.; Fujita, T.; Nangaku, M. Hypoperfusion of peritubular capillaries induces chronic hypoxia before progression of tubulointerstitial injury in a progressive model of rat glomerulonephritis. *J. Am. Soc. Nephrol.* **2004**, *15*, 1574–1581. [[CrossRef](#)] [[PubMed](#)]
58. Hirakawa, Y.; Tanaka, T.; Nangaku, M. Renal hypoxia in CKD; pathophysiology and detecting methods. *Front. Physiol.* **2017**, *8*, 99. [[CrossRef](#)]
59. Fu, Q.; Colgan, S.P.; Shelley, C.S. Hypoxia: The force that drives chronic kidney disease. *Clin. Med. Res.* **2016**, *14*, 15–39. [[CrossRef](#)] [[PubMed](#)]
60. Erler, J.T.; Cawthorne, C.J.; Williams, K.J.; Koritzinsky, M.; Wouters, B.G.; Wilson, C.; Miller, C.; Demonacos, C.; Stratford, I.J.; Dive, C. Hypoxia-mediated down-regulation of Bid and Bax in tumors occurs via hypoxia-inducible factor 1-dependent and-independent mechanisms and contributes to drug resistance. *Mol. Cell. Biol.* **2004**, *24*, 2875–2889. [[CrossRef](#)] [[PubMed](#)]
61. Chen, J.; Zhao, S.; Nakada, K.; Kuge, Y.; Tamaki, N.; Okada, F.; Wang, J.; Shindo, M.; Higashino, F.; Takeda, K. Dominant-negative hypoxia-inducible factor-1 $\alpha$  reduces tumorigenicity of pancreatic cancer cells through the suppression of glucose metabolism. *Am. J. Pathol.* **2003**, *162*, 1283–1291. [[CrossRef](#)]
62. Dai, S.; Huang, M.L.; Hsu, C.Y.; Chao, K.C. Inhibition of hypoxia inducible factor 1 $\alpha$  causes oxygen-independent cytotoxicity and induces p53 independent apoptosis in glioblastoma cells. *Int. J. Radiat. Oncol. Biol. Phys.* **2003**, *55*, 1027–1036. [[CrossRef](#)]
63. Kang, D.-H.; Hughes, J.; Mazzali, M.; Schreiner, G.F.; Johnson, R.J. Impaired angiogenesis in the remnant kidney model: II. Vascular endothelial growth factor administration reduces renal fibrosis and stabilizes renal function. *J. Am. Soc. Nephrol.* **2001**, *12*, 1448–1457. [[PubMed](#)]
64. Agarwal, A.; Nick, H.S. Renal response to tissue injury: Lessons from heme oxygenase-1 gene ablation and expression. *J. Am. Soc. Nephrol.* **2000**, *11*, 965–973. [[PubMed](#)]
65. Vesey, D.A.; Cheung, C.; Pat, B.; Endre, Z.; Gobe, G.; Johnson, D.W. Erythropoietin protects against ischaemic acute renal injury. *Nephrol. Dial. Transplant.* **2004**, *19*, 348–355. [[CrossRef](#)] [[PubMed](#)]
66. Conde, E.; Alegre, L.; Blanco-Sanchez, I.; Saenz-Morales, D.; Aguado-Fraile, E.; Ponte, B.; Ramos, E.; Sáiz, A.; Jiménez, C.; Ordoñez, A. Hypoxia inducible factor 1-alpha (HIF-1 alpha) is induced during reperfusion after renal ischemia and is critical for proximal tubule cell survival. *PLoS ONE* **2012**, *7*, e33258. [[CrossRef](#)]
67. Hill, P.; Shukla, D.; Tran, M.G.; Aragonés, J.; Cook, H.T.; Carmeliet, P.; Maxwell, P.H. Inhibition of hypoxia inducible factor hydroxylases protects against renal ischemia-reperfusion injury. *J. Am. Soc. Nephrol.* **2008**, *19*, 39–46. [[CrossRef](#)] [[PubMed](#)]
68. Danobeitia, J.S.; Djamali, A.; Fernandez, L.A. The role of complement in the pathogenesis of renal ischemia-reperfusion injury and fibrosis. *Fibrogenesis Tissue Repair* **2014**, *7*, 1–11. [[CrossRef](#)]
69. Kapitsinou, P.P.; Jaffe, J.; Michael, M.; Swan, C.E.; Duffy, K.J.; Erickson-Miller, C.L.; Haase, V.H. Preischemic targeting of HIF prolyl hydroxylation inhibits fibrosis associated with acute kidney injury. *Am. J. Physiol. Ren. Physiol.* **2012**, *302*, F1172–F1179. [[CrossRef](#)]

70. Yang, S.-Y.; Pyo, M.C.; Nam, M.-H.; Lee, K.-W. ERK/Nrf2 pathway activation by caffeic acid in HepG2 cells alleviates its hepatocellular damage caused by t-butylhydroperoxide-induced oxidative stress. *BMC Complementary Altern. Med.* **2019**, *19*, 1–13. [[CrossRef](#)] [[PubMed](#)]
71. Li, W.; Turner, A.; Aggarwal, P.; Matter, A.; Storvick, E.; Arnett, D.K.; Broeckel, U. Comprehensive evaluation of AmpliSeq transcriptome, a novel targeted whole transcriptome RNA sequencing methodology for global gene expression analysis. *BMC Genom.* **2015**, *16*, 1–13. [[CrossRef](#)]
72. Huang, D.W.; Sherman, B.T.; Lempicki, R.A. Bioinformatics enrichment tools: Paths toward the comprehensive functional analysis of large gene lists. *Nucleic Acids Res.* **2009**, *37*, 1–13. [[CrossRef](#)] [[PubMed](#)]
73. Liberzon, A.; Birger, C.; Thorvaldsdóttir, H.; Ghandi, M.; Mesirov, J.P.; Tamayo, P. The molecular signatures database hallmark gene set collection. *Cell Syst.* **2015**, *1*, 417–425. [[CrossRef](#)]